FACULTAD DE CIENCIAS DEL MAR

UNIVERSIDAD DE LAS PALMAS DE GRAN CANARIA

Study of the seismic-tidal correlations for pre-eruptive, eruptive and post-eruptive stages of the submarine volcano Tagoro, El Hierro Island.

Atenary Pimentel González

Curso 2016/2017

Dr. Eugenio Fraile Nuez

Prof. Dr. Melchor González Dávila

Trabajo Fin de Título para la obtención del título de Grado en Ciencias del mar.

Study of the seismic-tidal correlations for pre-eruptive, eruptive and post-eruptive stages of the submarine volcano Tagoro, El Hierro Island.

Student: Atenary Pimentel González.

Grado en Ciencias del Mar.

Curso: 2016-2017.

Universidad de las Palmas de Gran Canaria, Facultad de Ciencias de Mar.

Proyecto realizado en el Centro Oceanográfico de Canarias (COC), Instituto Oceanográfico Español (IEO).

Tutor: Prof. Dr. Melchor González Dávila.

Departamento de Química, Universidad de las Palmas de Gran Canaria, Las Palmas de Gran Canarias, España.

Instituto Universitario de Oceanografía y Cambio Global (IOCAG)

UNIVERSIDAD DE LAS PALMAS DE GRAN CANARIA
Instituto Universitario de Oceanografía
y Cambio Global

IOCAG

Co-tutor: Dr. Eugenio Fraile Nuez

Instituto Español de Oceanografía (IEO), Centro Oceanográfico de Canarias (COC).38180 Santa Cruz Tenerife, España.

INSTITUTO ESPAÑOL DE OCEANOGRAFÍA

Atenary Pimentel González.

Santa Cruz de Tenerife, a 6 de Julio 2017

Prof. Dr. Melchor González Dávila

Las Palmas de Gran Canaria, a 6 de Julio 2017

Dr. Eugenio Fraile-Nuez

Santa Cruz de Tenerife, a 6 de Julio 2017

Index

Atenary Pimentel González.

1. Abstract

During the seism-eruptive process that took place at the island of El Hierro (Canary Islands) between 01/01/2011-31/07/2012, more than 15,000 earthquakes distributed during the different stages (pre-eruptive, eruptive and post-eruptive), were registered. This eruptive process gave the opportunity to analyze the possible existence of any relation between earthquakes and tide for each of the stages of the process. In order to verify that, several earthquakes swarms were selected from each stage. Subsequently, each swarm was subjected to different spectral analysis techniques. The results obtained in this work, demonstrated the existence of a strong influence of the tide with earthquakes, especially in the pre-eruptive stage and the reactivation swarm of the post-eruptive stage. It is also noteworthy, that the influence of the semi-diurnal tide respect to the probability of occurrence of earthquakes is more significant than the diurnal tide. Moreover, this study also demonstrated the existence of higher occurrence of earthquakes during events of low tide with respect to high tide.

Keywords: Earthquakes, tide, correlation, El Hierro Island, Canary Island.

2. Motivation

The capacity or probability of being able to predict an earthquake, either individually or on a statistical base is very low. The prediction during a seismic crisis of a moment or moments in which earthquakes are going to occur is really important, not only for the demarche of the crisis itself but also for the probability of minimize the disastrous effects in the society and properties.

This study expects to advance in the scientific knowledge in order to help in the difficult task of the prediction of earthquakes or in the determination of those statically significant moments in which a large number of earthquakes could produce more damages.

For this study we will investigate the possible correlation between the ocean tide component and the occurrence of seismic events. For future works we would like to investigate other physical components that increase predictive probability as atmosphere pressure, Moon phase, Sun phase, etc.

3. Background

The shallow submarine eruption which took place in 10/10/2011 occurred at 1.8 km south of the Island of El Hierro, the youngest Island of the Canary Islands. The submarine volcano begins on the S-ridge at 350 m depth and rise to 88 m below sea level (Fraile-Nuez et al., 2012; Santana-Casiano et al., 2013). The eruptive event was preceded by a strong seismic crisis that began approximately on 17^{th} of July of 2011, during which the National Geographic Institute (IGN) registered approximately 10,000 earthquakes ($M \leq 4.3$) that were migrated by swarms from the north to the south of the Island. The eruptive process finished off 05/03/2012, given rise the hydrothermal system (Fraile-Nuez et al., 2012; Santana-Casiano et al, 2013) with different seismic reactivations stages that were register by IGN.

This event is the first eruptive phenomenon in the last 40 years in Spain and, it was an unprecedented phenomenon for the Spanish oceanography. Oceanography made volcano an object to multidisciplinary study. So, the eruptive process made numerous studies in the area affected by the underwater eruption, this is because the volcano transformed that area (El Mar de las Calmas) in a natural laboratory. Because the volcano emission react with seawater leading to important physical-chemical anomalies that may strongly impact the marine ecosystem (Hall-Spencer et al., 2008; Resing et al., 2009). Fraile-Nuez et al. (2012) observed the different anomalies in the physical-chemical parameters caused during the eruptive process of the Tagoro volcano. During this eruptive process Fraile-Nuez et al. (2012) observed that the emission of the volcano produced anomalies in temperature and salinity of +0.3ºC and -0.3, respectively, at 80 m depth and 290 m from the volcano, even getting to registered anomalies of temperature of +18.8ºC over the crater at 210 m depth. The volcano emit CO_2, and this produced total inorganic carbon concentration ranging from 4,000 to 7,500 µmol kg^{-1} producing a water acidification of up to 2.8 units in the first 100 m depth and 2 km of the volcano. The increase of CO_2 levels generated high partial pressure of CO_2 (pCO_2) with values ranging from 12,000 to 150,000 µatm at the surface. The part of the column of water most affected by the Tagoro volcano was between 75 and 125 m, in which experimented anoxia levels, negative redox potential, pH decrease, maximum concentrations of reduced sulfur (200 µmol kg^{-1}) and total Fe (II) (50 µmol kg^{-1}) and higher concentrations of dissolved Cu, Cd, Pb and Al with maximum values of 6.1, 6.7, 5.8 and 2,122 nM, respectively. These anomalies produced by the volcano caused the dead of fishes and that the vertical migration was rather weak or absent as a consequence of anoxic levels in shallow layers (Fraile-Nuez et al., 2012). These anomalies were also observed by Santana-Casiano et al. (2013) the same anomalies and they observed that the abrupt changes in the physical-chemical properties of the sea water composition, producing an unprecedented of severe acidification and fertilization.

It is noteworthy, that these anomalies continued after the end of the eruptive process and continued to produce anomalies associated with the hydrothermal system that originated after the submarine eruption. Being found two years after the volcanic eruption have registered negative anomalies of pH observed in the area, including values as high as −0.25, cannot be explained by the arrival of water from the surrounding depths (Santana-Casiano et al., 2016). The pH value of 7.89 in the volcano area is found in the non-affected surrounding water at a depth of 900 m (Santana-Casiano et al., 2016).

4. Introduction

Seismicity at volcanoes has been proposed to be correlated with earth tides (Mauk and Johnston, 1973; Dzurisin, 1980; Rydelek, et al., 1988), and the influence of tides on seismicity in general has been debated for many years (Omori, 1908). Some studies have shown the correlation between tidal forces, earthquakes and volcanos eruptions as in Tolstoy et al. (2002), for the Axial Seamount volcano in Juan la Fuca plate. The studies of Glaser (2003) added more information to this correlation by demonstrating that when the tidal forces are strongest, earthquake and volcanic eruptions are the most severe. These tides, coinciding with the days of full moon or new moon, the tidal forces of the Moon and the Sun are in concert (Glaser, 2003), this is when there is an alignment between the three bodies. In addition, the perigee coincides within a day o two day of new Moon or full Moon, when the tidal effects are further reinforced (Glaser, 2003).

Correlations between seismicity and tidal stress are statistically significant but, generally limited to special regions or circumstances (Ide et al., 2016). Some examples were of great influence regarding the topic, such as the great earthquake Tohoku–Oki (Ide et al., 2016) in Japan and the Axial Seamount volcano in the pacific plate (Tolstoy et al., 2012) In the last case, correlations were only found for earthquakes of magnitude higher than 6 (Tolstoy et al., 2002). Tidal influence has been observed in earthquakes and eruptions associated with plate boundaries as in the study of the Pavlof volcano in Alaska, in which it was observed that the correlation changes during the course of the eruption of 1974, in this eruption was observe that during the pre-eruptive earthquakes swarms occurs during the compression tide, while in the post-eruptive swarms occurs during the increasing tide extension (Mcnutt & Beavan, 1981). It is also worth mentioning that Rydelek et al. (1988), demonstrated the correlation between tide and earthquakes produced by the Kilauea volcano, in Hawai'i. In this case, this correlation is for islands associated with hot spots.

Most studies with earthquake catalogs have demonstrated the existence of this strong correlation between earthquake and tide generation (Schuster, 1897; Morgan et al., 1961; Simpson, 1967; Heaton, 1982; Curchin & Pennington, 1987; Hartzell & Heaton, 1989), but there are also studies that reject this correlation (Heaton, 1975; Ding et al., 1983; Tsuruoka et al., 1995). In addition, some of the studies carried out not only confirm the existence of a strong influence of the tide on earthquakes but also have shown that the influence of low tide is much higher than that of high tide, they have observed that during the low tide produces a greater number of earthquakes (Tolstoy et al., 2002 ; Wilcock, 2001). In addition, Wilcock (2001) it not only observes that the occurrence of earthquakes is greater at low tide, but increase at low tides that occur during the spring.

The main purpose of the present study is the determination of the possible tidal influence on the earthquakes that took place by the monogenetic submarine volcano of El Hierro Island, Tagoro. After a brief presentation of the previous knowledge in the study, the material and methods used were explained. After this, a results section has been presented to finally arrive to the discussion and conclusion section.

5. Material and methods

Earthquake catalogue: A catalogue of earthquake with location and local magnitude (mbLg) for the whole Canary Island Archipelago was obtained from the National Geographic Institute (IGN). The catalog spans the time interval since 01/01/2011 until 31/07/2012. In this period of time, the IGN register 15,423 earthquakes, of which 15,268 occurred in the vicinity of El Hierro Island (Figure 1).

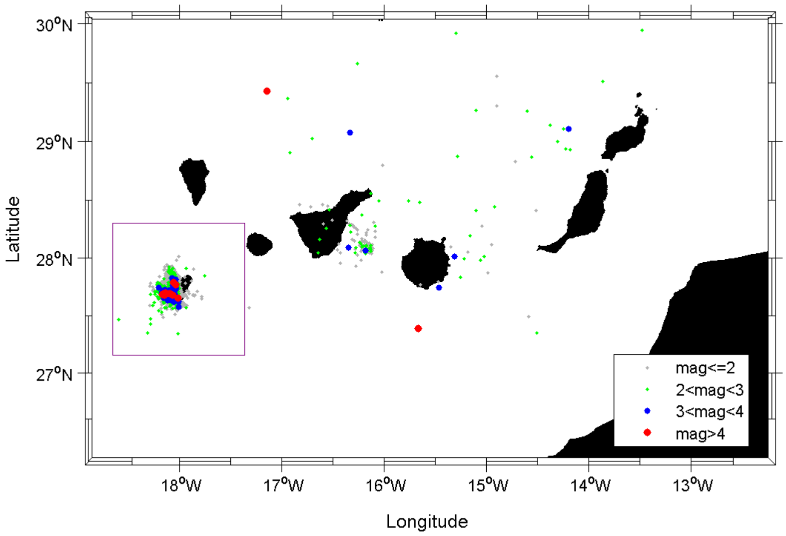

Figure 1: Map of the earthquakes registered at the Canary Islands during 2011-01-01 until 2012-07-31. Earthquakes magnitudes are presented in different colors.

In order to analyze the earthquake data, the database was equal-spaced in hours, and the vectorization of the earthquakes was performed in order to group them by hours. After this, it was applied three filters to eliminate noise from the time series of earthquakes. The first and second filter, that were used by Ridelek et al. (1988), this filter were use to eliminate high frequencies (smooth) and low frequencies (second-order polynomial function). Finally, the third filter was applied that considers the first derivate used to emphasize the filtering. The random earthquakes data is not significantly biased by these numerical filters

Sea level height data: The tidal used in this study was an estimated tidal obtained by a TPXO7.2ATLAS tidal ocean model (Egbert, Bennett, & Foreman, (1994). TOPEX / POSEIDON). This model produces tide estimations with different principal constituents. In our case, a tidal with the main constituents as M_2 (harmonic semidiurnal forcing of Lunar origin), S_2 (harmonic forcing of solar origin), K_1, and O_1 (diurnal components) and the secondary constituents showed in Table 1. For this study, it was estimate the tide with intervals of one hour between each data for the period of time in which the study was conducted, from 01/01/2011 to 31/07/2012.

Table 1: Periods and amplitudes of the different tidal constituents.

Constituents	Description	Period (hours)	Amplitude(m)
M_2	Principal lunar semidiurnal constituent	12.42	0.6
S2	Principal solar semidiurnal constituent	12	0.24
O1	Principal lunar declinational diurnal constituent	25.82	0.04
K1	Luni-solar declination diurnal constituent	23.93	0.06
N2	Larger lunar elliptic semidiurnal constituent	12.66	0.12
P1	Principal solar declinational diurnal constituent	24.07	0.016
K2	Luni-solar semidiurnal constituent	11.96	0.06-0.08
Q1	Larger lunar elliptic constituent	26.87	0.15
M4	Shallow water over tides of principal lunar constituent	6.21	--
MF	Luni-solar fortnightly constituent	327.87	--
MM	Lunar monthly constituent	661.76	--
MS4	Shallow water quarter diurnal constituent	6.10	--
MN4	Shallow water quarter diurnal constituent	6.27	--

Fast Fourier Transform (FFT): The FFT (Cooley & Tukey, 1965; Rader, 1968; Oppenheim & Schafer, 1989; Duhamel & Vetterli, 1990; Frigo & Johnson, 1998) is a mathematical method that extracts the periodic or harmonic frequencies of a signal. The FFT could be defined by the following linear summation**:**

$$y = \frac{1}{2}A_0 + \sum_i^x [A_i \cos(\varpi_i t) + B_i \sin(\varpi_i t)] \quad (1)$$

In which A_0 is the mean value of the record, A_i and B_i are constants or amplitude of the harmonic wave (Fourier coefficients), ϖ_i is the specific angular frequency, and t is the time variable.

The FFT extracts the harmonic or periodical signals and transform them in cycles of a certain frequency and with a certain degree of significance. In addition, as this model allows extract significant wave or periods with which could be realized a reconstruction of the original signal. The number of waves used to perform a reconstruction close to the original will depend on the signal to be studied.

The original FFT method works just for series completely equispaciated and with no gap on it. Our time series of earthquakes is some where random and with gaps, therefore a modified methodology of a FFT (Fastlomb, Lomb (1976); Press et al, 2001) was applied. Moreover, this methodological variant has its own significance test with different significance levels, from 0.9 the lowest to 0.999 over 1.

Wavelet: The CWT, Continuous Wavelet Transform (Torrence & Compo, 1998; Grinsted et al., 2004), is an alternative method to extract a significative or harmonic period of a signal. The wavelet is a method applied for the analysis of signals, which allows us not only to obtain significant cycles or periods in the range of the frequencies but also in the time-frequency space. This new information allowed to determinate if the signal has intermittent periods, or in which parts of the study timeline the signal is significant.

Reconstruction: Ones the fastlomb has been applied to the time series and the significant frequencies or harmonious signal have been obtained, these periods are used to reconstruct the filtrated original signal. For the reconstruction of the filtered signal only the harmonized periods obtained in the fastlomb that had a greater explained variance and that are within the tidal range both semidiurnal and diurnal were taken into account. The analysis and processing of the data have been done under Matlab computation and following the equation (1).

Matlab: All data analysis and processing was performed under the Matlab environment. To carry out this analysis and processing of the data, specific toolboox were applied for studies in the oceanographic field. Maping generations by m_map toolbox by Rich Pawlowicz for Department of Earth and Ocean Sciences of University of British Columbia. Theoretical tide by TOPEX tide model by Egbert and Erosfeeva, COAS and OSU Disclaimer for the National Science Foundation, the Office of Naval

Reseach and the National Aeronautics. Fastlomb analysis by Saragiotis in 2008 and Wavelet analysis by Alask Grindsted from 2002-2004 for the National Oceanographic Center in Liverpol.

6. Results

6.1. Earthquakes catalog

A total of 15,423 earthquakes were registered at the Canary Islands with magnitudes between 0 and 5 of which 15,268 earthquakes were considered in this study because they took place at the vicinity of the El Hierro Island.

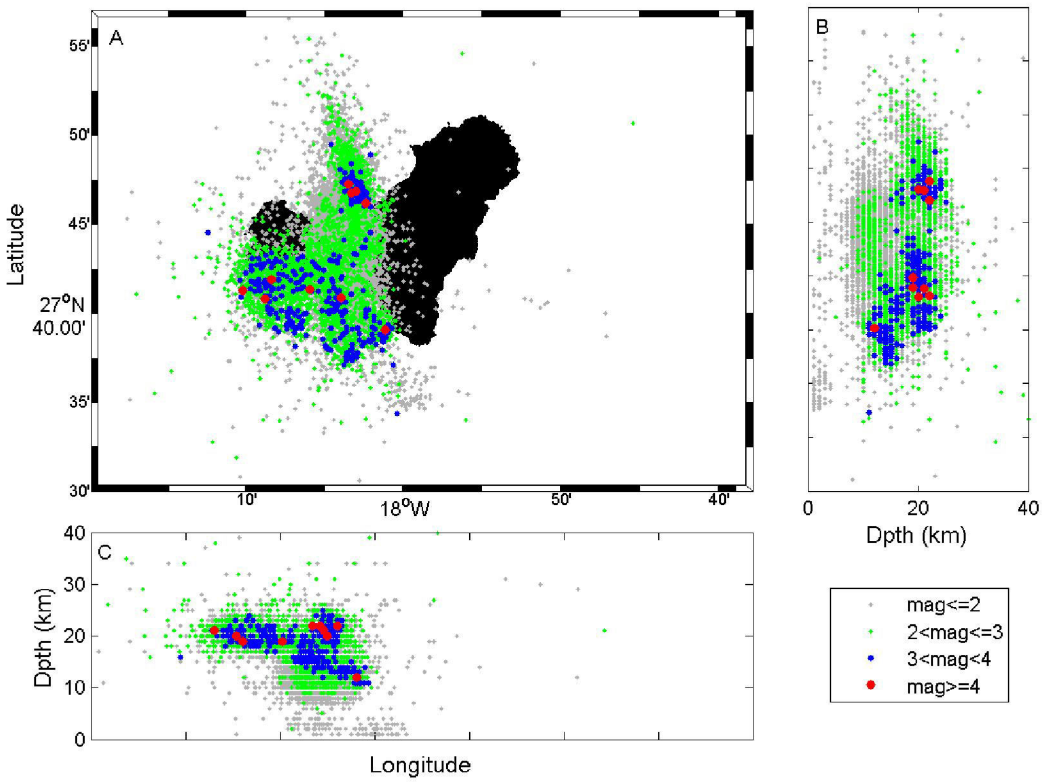

Figure 2: Map of earthquake that took place at the El Hierro Island. (A) Locations of earthquake registered in El Hierro Island during the calm, pre-eruptive, eruptive and post-eruptive stages. (B) Positions of earthquakes respect depth (km) and latitude (°). (C) Locations of earthquakes respect longitude (°) and depth (km).

Figure 2 shows the location of the 15,268 earthquakes produced between 01/01/2011 to 31/07/2012 together with the magnitude and depth/latitude/longitude plots at El Hierro Island. Figure 2 A represents the different earthquakes by magnitudes and colors with a total of 11966 events for magnitudes between 0-2, 3037 events for 2<m<=3, 255 events for magnitudes between 3<m<4 and 10 earthquakes for magnitudes equal or higher than 4.

Figures 2 B and 2 C, show the depth where seismic events were generated. Most earthquakes were produced between 10-30 km depth. The earthquakes in the range of 4-5 of magnitude were originated at 20 km depth, except one, that occurred at a depth of 10 km. Earthquakes generated in surface (0-10 km depth) correspond to the earthquakes with smaller magnitude.

This time series of earthquakes has been divided into 4 different stages related to specific seismic-volcanic events. The first stage corresponds with the calm stage from 01/01/2011 to 20/07/2011. At the end of July, the pre-eruptive stage started on 21/07/2011, concluding when the magmatic activity took place on 10/10/2011. The magmatic stage was active for more than 5 months until 05/03/2012. After finishing the eruptive process, the volcano became a hydrothermal system with different stages of seismic reactivation. For this study, only the first stage of reactivation, from 24/06/2012 to 13/07/2012, has been analyzed.

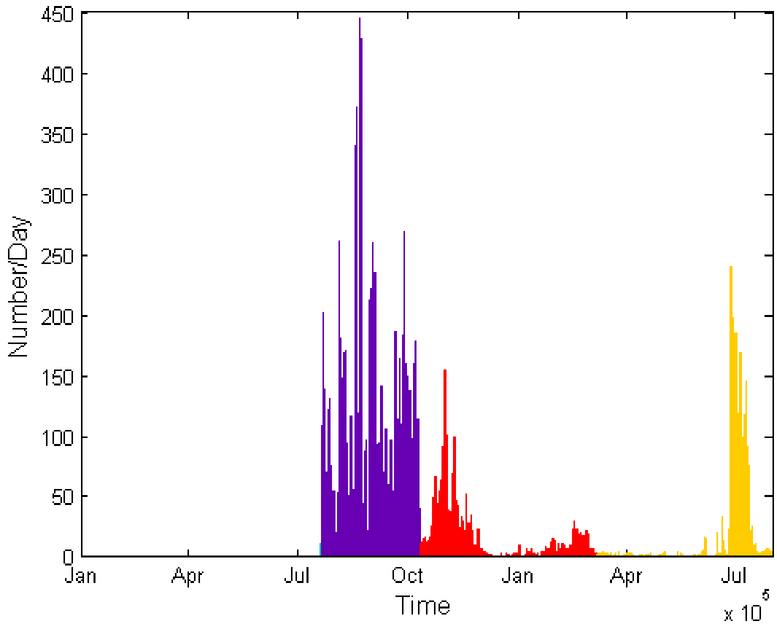

Figure 3: Time series of number of seismic events per day during the different stages of seism-eruptive process of El Hierro Island. The different stages are represented by colors: calm in light blue, the pre-eruptive in blue, the eruptive in red and the post-eruptive in yellow.

Figure 3 shows the earthquakes that occurred at El Hierro Island, during the period of study together with the relation of those earthquakes with the tide. Figure 3 A shows a bar diagram, which presents the number of the earthquakes per day that took place in the different stages. Therefore, it reflects the seismic activity of the different stages.

During the pre-eruptive stage an important seismic activity took place. In this stage, 9990 earthquakes, even reaching 444 earthquakes in a day, occurred. In the eruptive stage the number of earthquakes decreased compared with the previous stage with a total of 2587 events. Most of these seismic events occurred in the first two months of the stage, where 1962 earthquakes were recorded. During the post-eruptive phase there was a period of time with a low seismic activity from 05/03/2012 to 31/07/2012 but suddenly, a reactivation phase took place from 24/06/2012 until 13/07/2012 with a total of 2338 seismic events.

These four different stages have been divided in different swarms where seismic events occurred continuously in time and centered in almost the same place.

Figure 4 show the different swarms of each stage that were registered during the period the time that was analyzed in this study. Figure 4 A shows the map of earthquakes locations that occurred during 01/01/2011 to 20/07/2011 (calm stage). Seismic activity at this stage was almost non-existent, with only 19 earthquakes recorded during the entire stage.

Figures 4 B, C and D show the earthquake swarms that took place in the pre-eruptive stage. These swarms presented significant changes in the position of the earthquakes events during the stage. For the figures 4 B and C shows the swarms that occurred from 21/07/2011 to 12/08/2011 and from 14/08/2011 to 23/08/2011 respectively. These swarms the concentration of earthquakes is located in the North West of the island, while in the figure 4 D that present the swarm that took place between 24/08/2011 and 10/10/2011. In this swarm the location of earthquakes are distributed from the north to the south of the island.

The Figures 4 E and F show the swarms for the earthquakes locations that took place in the eruptive stages. In this stage, seismic activity ceased as the submarine eruption progressed in time. So, the Figure 4 E present the swarm that were occur from 10/10/2011 to 09/12/2011, and this figure presented a greater seismic activity than the swarm that represented in the Figure 4 F, this swarm occurred from 17/01/2012 to 05/03/2012. In the eruptive stage, the swarms presented changes in the positions. The earthquakes location for the swarm of the Figure 4 E was more concentrated in the north part of the island, while in the swarm of the Figure 4 F the earthquakes had migrated to the south of the island

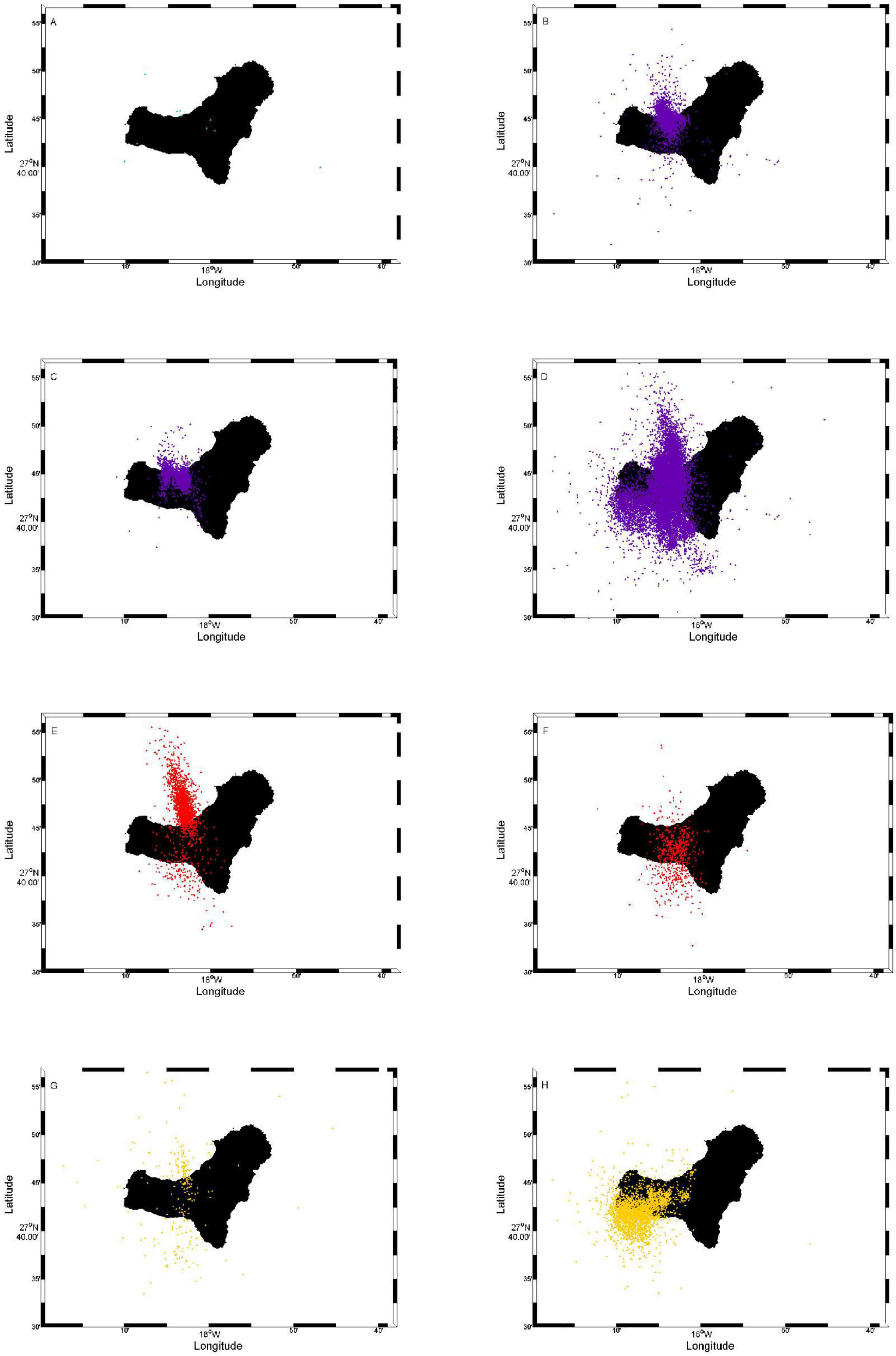

Figure 4: Maps of earthquake locations from different swarms at the different stages. (A) Swarm of earthquakes of the calm stage (light blue). (B, C and D) Swarms of earthquakes of the pre-eruptive stage (blue). (E and F) Swarms of seismic of the eruptive stage (red). (G and H) Swarms of earthquakes of the post-eruptive stages (yellow).

The Figures 4 G and 4 H show earthquake's swarm locations that took place in the post-eruptive stage. The Figure 4 G present the swarm that occurred from 5/03/2012 to 23/06/2012 and this swarm has a significant lower seismic event that‘ swarm that took place from 24/06/2012 to 13/07/202 (Figure 4 H) and that is due to this last swarm coincides in time with the first reactivation that it is present in the Figure 3 in the post eruptive stage (yellow). The position of the seismic events were distributed in different coordinates, swarm of Figure 4 G located form north to south of the island, while swarm of the Figure 4 H concentrated in the south west of the island.

6.2. Ocean Tide

Ocean tide is the principal physical variable to be correlated with the seismic event in this study. As indicated in the material and method section, the tide used in this study has been estimated as the tidal obtained by a TPXO7.2ATLAS tidal ocean model (Egbert, Bennett, & Foreman, (1994). TOPEX / POSEIDON) with all tidal constituents showed in Table 1.

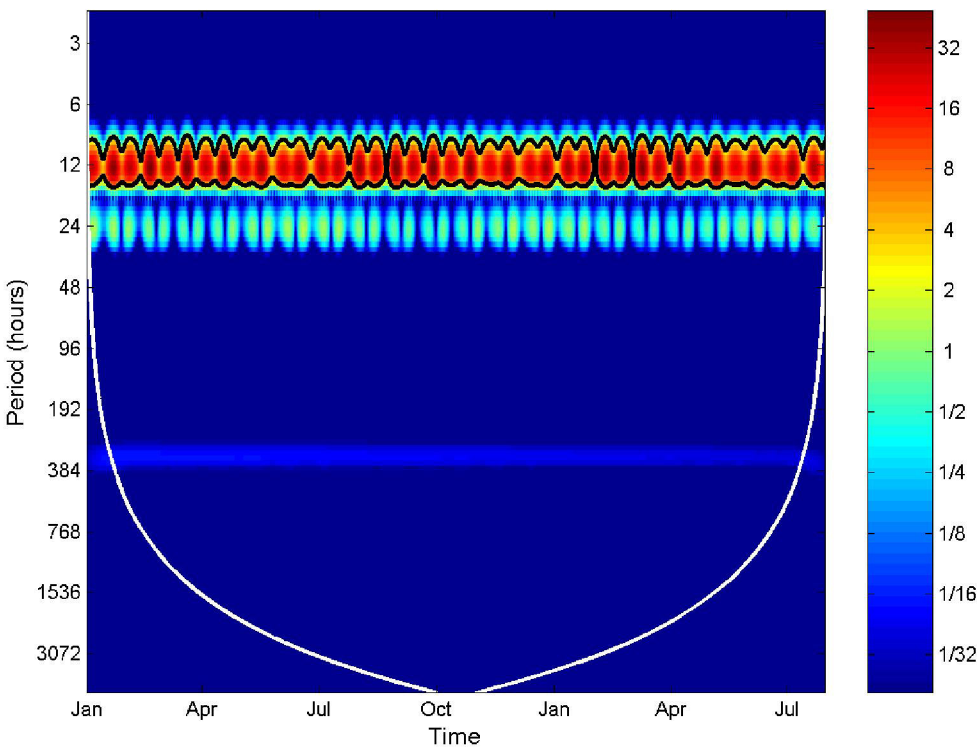

Figure 5: The continuous wavelet power spectrum applied to the modeled tidal with its different components (M_2, S_2, K_1, O_1, N_2, P_1, K_2, Q_1, M_4, MF, MM, MS_4, MN_4) for the period of time of the study. The white line is the significance level at 95%. The thick black contour represents the power spectrum with significance higher than 95%.

Figure 5 shows the tidal power spectrum generated by the wavelet analysis. The power spectrum obtained shows that the period of the semidiurnal tide reaches its maximum significance peak at 12 h while the diurnal period is centered around 24 h. The range of period for the semidiurnal tide at significance of 95% is between 8.9-15 h. Although the diurnal tide is also presented in the spectrum, it did not show significance as high as the semidiurnal component. The ranges of the diurnal period, varies from 18-30 h.

6.3. Earthquakes catalogues and ocean tide

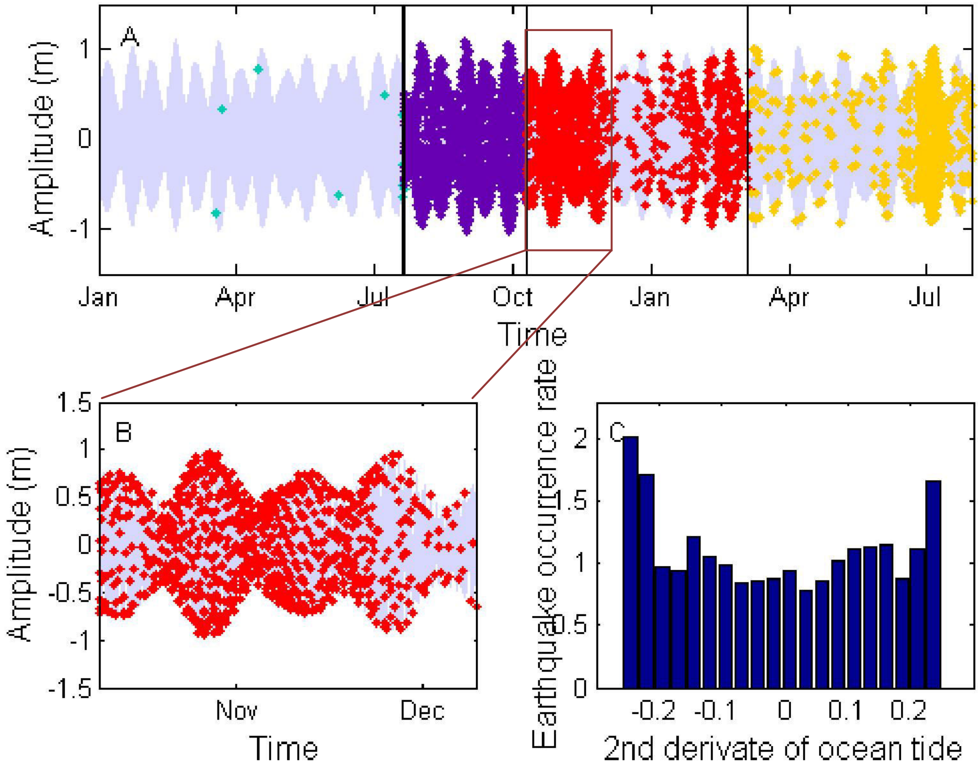

Figure 6: Relation between earthquakes and tide. (A) Present the distribution of earthquake versus the tidal amplitude to all stages. The different stages are represented by colors: calm in light blue, the pre-eruptive in blue, the eruptive in red and the post-eruptive in yellow. (B) Earthquakes position in the ocean during the first swarm (E1) of the eruptive stage. (C) Normalized histogram of earthquakes occurrence rate, with relatives to second derivate of ocean tide the first swarm (E1) of the eruptive stage.

Figure 6 presents the existing relationship between earthquakes and tide for the E1 earthquake swarm. Figure 6 A shows the temporal distributions of earthquakes respect to the tidal amplitude, showing the sea level height at which each seismic events occurred. Whereas the Figure 6 B shows the position of earthquakes at tidal amplitude for swarm E1. In this figure a strong relationship of earthquakes is observed with both low and high tide. This strong correlation between low and high tide with earthquakes is confirmed in Figure 6 C. This figure presents a normalized histogram of the relative occurrence of earthquakes versus the second derivative of the oceanic tide. When applying the second derivative to perform this correlation analysis between the tide and the earthquakes, it was obtained that the negative amplitudes correspond to the high tide while the positive amplitudes with respond with the low tide.

This figure shows that there is a greater accumulation of earthquakes in the ends of the graph, that is to say a greater number of earthquakes occurs when the maximum and minimum of tide are produced. But it is noteworthy that although there are a great part of earthquakes when there is high tide, the relationship between low tide and earthquakes is stronger as there are a greater number of earthquakes near the minimum tide.

6.4. Spectral analysis

In order to determinate the possible influence of the tide on earthquakes, a spectral analysis has been applied to the swarms that appear in Figure 4. These swarms will be denominated as C_1 (Figure 4 A) for calm stage, Pre1 (Figure 4 B), Pre_2 (Figure 4 C) and Pre_3 (Figure 4 D) for pre-eruptive stage, E_1 (Figure 4 E) and E_2 (Figure 4 F) for eruptive stage and finally, P_1 (Figure 4 G) and P_2 (Figure 4 H) for post-eruptive stage.

Figure 7 shows the possible influence of the tide on the 5588 earthquakes occurred at the swarm Pre3, during the pre-eruptive stage. Figure 7 A shows a bar diagram, with the number of seismic events per hour. The position of these earthquakes in terms of tidal amplitude and time is shown in Figure 7 B. A strong relationship between the tide and the generation of earthquakes can be detected. Figure 7 C, represents the Continuous Wavelet Transform (CWT). This methodology was applied to the filtered time series of earthquakes events. The wavelet analysis returned a spectrum that shows the significant periods of the series with time, which are represented with a significance level of 95%. In this figure shows the semidiurnal and diurnal component containing filtered from earthquakes, these tidal components are reflected in significant periods with a determined duration of time. The harmonic periods extracted by the CWT are centered around 12 h coinciding with the semidiurnal tide period. In some swarms, not only are significant cycles related to semidiurnal tides, but also to the diurnal tide (24 h) is observed (Table 2).

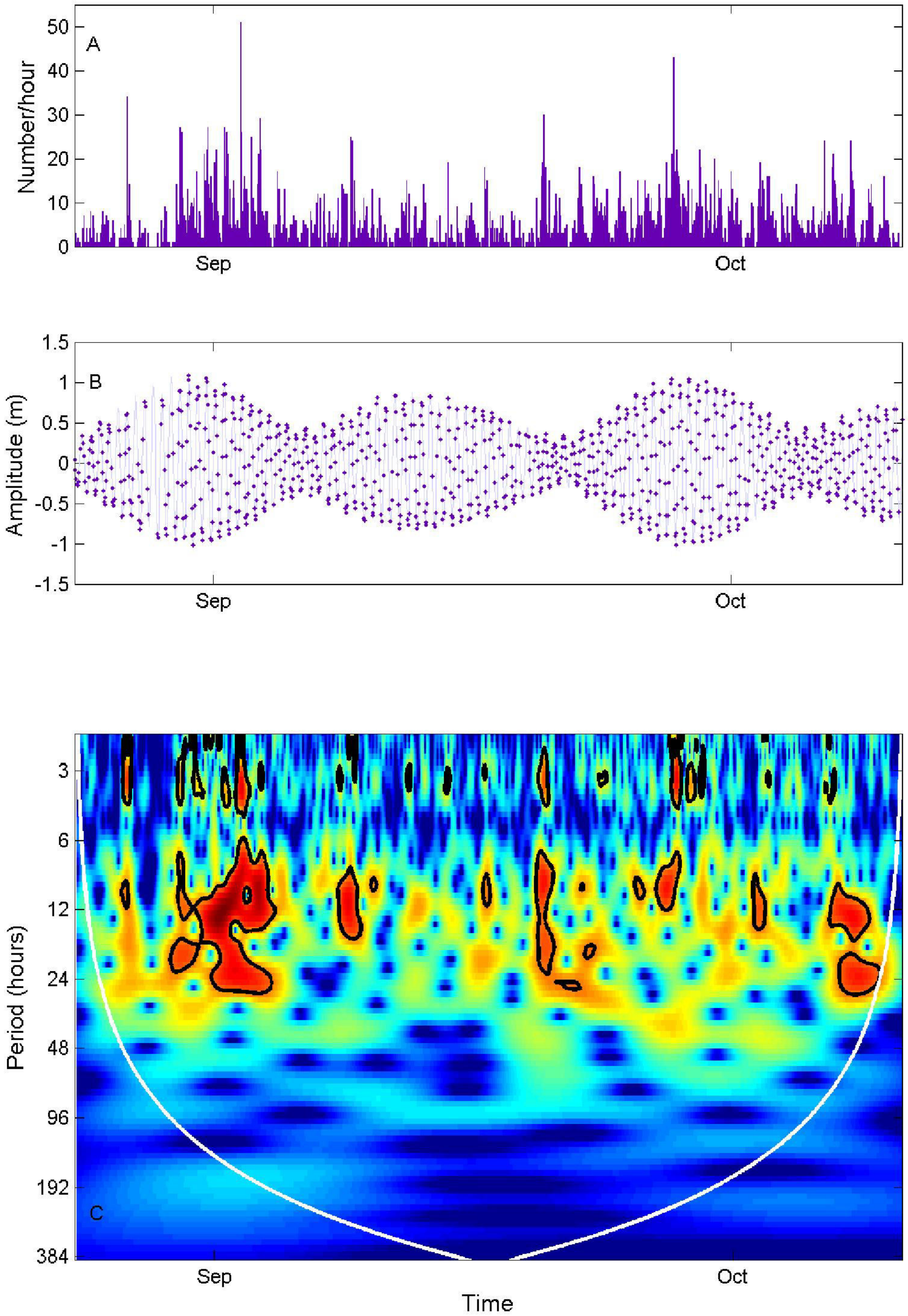

Figure 7: (A) Time series showing the number of seismic events per hours in pre-eruptive stage (swarm 21/07/2011 until 12/08/2011), (B) distribution of earthquake positions within the tidal amplitude (m). (C) Result of the application of the wavelet analysis to the filtered time series.

Table 2 presents, for all the stages studied, the most representative significant period at each swarms, sorted by magnitudes. It also shows the number of events produced in each swarm by magnitudes, and the percentage of reconstruction of the signal with the most important periods.

Table 2: Periods and significance of the significant harmonic component resulting from the spectral analysis. Moreover, the percentages of reconstructions of the original signal with these harmonic frequencies are shown. SD refers to semidiurnal tide and D refers to diurnal tide.

Period		**Magnitude**	**Earthquake number**	**Significative period**		**Significance**	**Reconstruction (%)**
Calm	**C_1 2011-01-01 2011-07-20**	M>0	19	--	--	--	--
		M>1	19	--	--	--	
		M>2	5	--	--	--	
		M>3	0	--	--	--	
		M>4	0	--	--	--	
Pre-eruptive	**Pre_1 2011-07-21 2011-08-12**	M>0	2273	12.7	SD	>0.999	34
				14.8		>0.999	
				29.5	D	0.999	
		M>1	1726	12.8	SD	0.95-0.995	37
				14.8		>0.999	
				29.5	D	0.95	
		M>2	59	11.2	SD	0.95	18
		M>3	0	--	--	--	--
		M>4	0	--	--	--	--
	Pre_2 2011-08-14 2011-08-23	M>0	2090	12.5	SD	0.95-0.995	35
				14.5			
		M>1	1017	12.4	SD	0.995	*38*
				14.5		0.95-0.995	
				20.8	D	0.9	
		M>2	18	13.6	SD	0.95	26
		M>3	0	--	--	--	--
		M>4	0	--	--	--	--
	Pre_3 2011-08-24 2011-10-10	M>0	5588	12.0	SD	>0.999	22
				24.2	D	0.95-0.995	
		M>1	3671	10.2	SD	0.90	10
		M>2	984	13.1		0.90	11
		M>3	75	--	--	--	--
		M>4	1	--	--	--	--

Continuation table 2

Period		Magnitude	Earthquake number	Significative period		Significance	Reconstruction (%)
Eruptive	**E$_1$ 2011-10-10 2011-12-09**	M>0	1962	11.4	SD	0.995	17
				26.4	D	0.95	
		M>1	1906	11.5	SD	0.995	17
				26.6	D	0.95-0.995	
		M>2	762	11.3	SD	0.95-0.995	13
		M>3	63	--	--	--	--
		M>4	4	--	--	--	--
	E$_2$ 2011-12-17 2012-03-05	M>0	578	10.4	SD	0.95	10
		M>1	344	10.9	SD	0.995	15
				9.9		0.90	
		M>2	26	11.8	SD	0.9	11
		M>3	1	--	--	--	--
		M>4	0	--	--	--	--
Post-eruptive	**P$_1$ 2012-03-05 2012-06-23**	M>0	237	10.3	SD	0.90	10
				14.0		0.95	
		M>1	153	10	SD	0.90-0.95	8
		M>2	14	10.2	SD	0.95-0.995	11
				13.8		0.90	
		M>3	0	--	--	--	--
		M>4	0	--	--	--	--
	P$_2$ 2012-06-24 2012-07-13	M>0	2338	11.6	SD	>0.999	42
				14.5		>0.999	
				18.1	D	0.95-0.995	
		M>1	2317	11.8	SD	>0.999	42
				14.5		0.999	
				18.3	D	0.95	
		M>2	1417	11.6	SD	>0.999	37
				14.6		0.999	
		M>3	124	--	--	--	--
		M>4	3	--	--	--	

The tidal components affecting the filtered series of earthquakes were not only analyzed by CWT, but analyzed with other spectral analyzes such as fastlomb in Hz (Table 1) and in cycles per day (Figure 8). The difference in performing the spectral analysis using the fastlomb in Hz is that the tide peaks were obtained with greater significance, while in the wavelet a tidal range was also obtained and a period of time in which the tide influenced the generation of earthquakes. Figure 8 A shows the spectrum obtained for the swarm Pre$_3$, after the accomplishment of a spectral analysis realized by the fastlomb method. In this graph, the significant optical periods shown in Table 2 are shown. Afterwards an analysis was also carried out in cycles per day since in this analysis the influence of the semidiurnal tide and of the diurnal tide on the earthquakes is clearly seen (Figure 8 B). This figure shows the peak with most significance in two cycles per day to swarm Pre_3. This peak has an approximate period of 12 h, which coincides with the semidiurnal tide component. In this figure, we also observe another peak with a great importance in one cycle per day, which has a period of 24 h coinciding with the diurnal tide component. In this figure was observed easier the correlation that exists between the earthquakes and the tide.

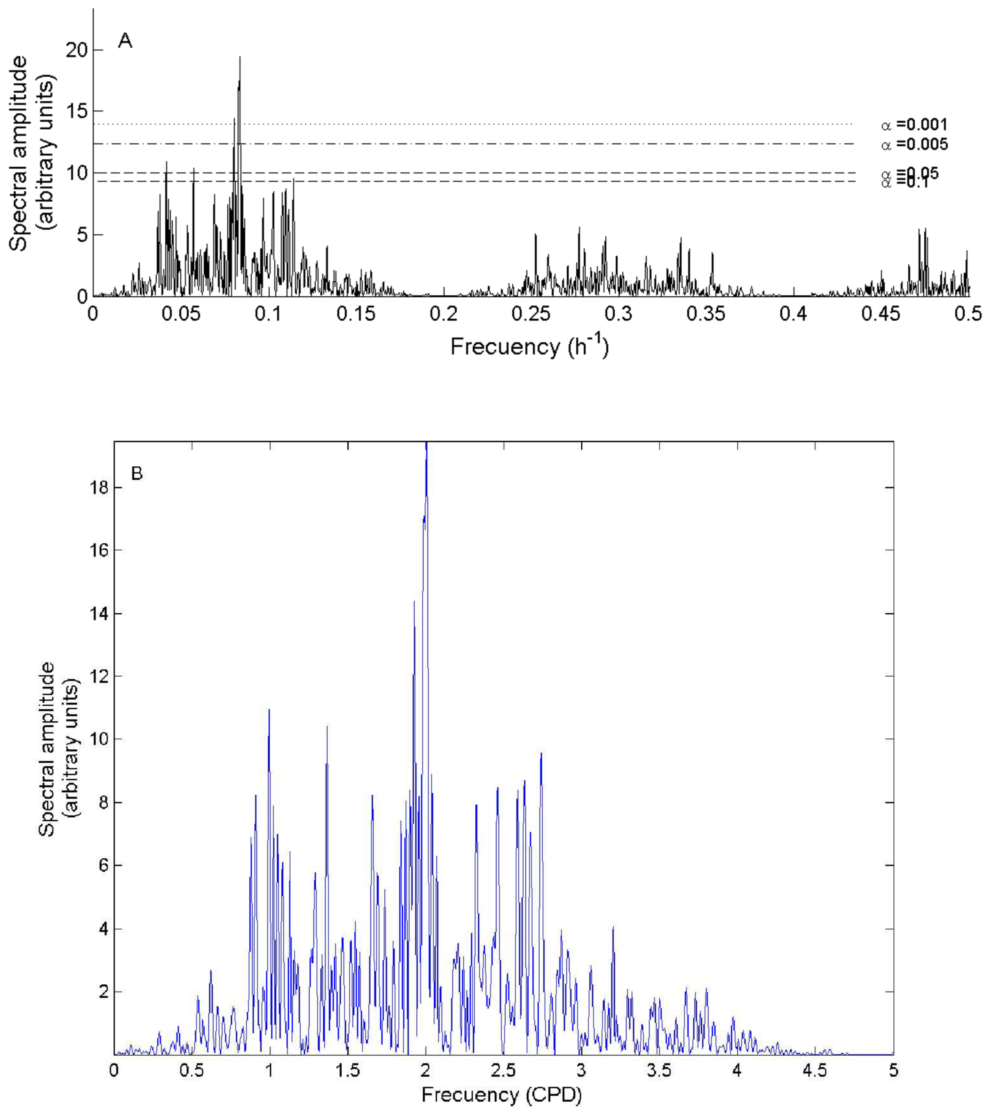

Figure 8: Spectral analysis by the fastlomb method. (A) Fastlomb spectral analysis in Hz with the different significant level and (B) Spectral amplitude in cycles per day (CPD) belonging to pre-eruptive swarms (2011/08/24 until 2011/10/10).

Figure 9 shows the influence of the tide on the 1962 earthquakes belonging to the first swarm of the eruptive stage (E_1). Figure 9 A shows the number per day of the earthquakes occurred during the first swarm of the eruptive phase. Figure 9 B shows the position of these earthquakes with respect to the amplitude of the tide in time. In this swarm, Pre_3, a strong relationship between the tide and the earthquakes can be detected.

Figure 9 C represents a Continuous Wavelet Transform (CWT), which returns significant harmonic periods for swarm E1. Most of these significant harmonic periods are centered around 12 h coinciding with the semidiurnal tide, but significant harmonic periods are centered also around 24 h which coincides with the diurnal tide. This figure shows a stronger relationship in the period of time that compares from the middle of October to the middle of November. While Figure 9 C shows the duration and the significant periods for swarm E_1, Table 2 shows the hours in which the tide has a greater influence on the earthquakes for swarm E_1. This swarm presents significant peaks with the semidiurnal tide in 11.4 h approximately, and in 26 h approximately to diurnal tide components. These results are observed for both magnitudes (m> 0 and m> 1), while for m> 2 only significant peaks coincide only with semidiurnal tide component.

Significant harmonic period for the E_2 and P_1 swarms do not show any coincidence with the diurnal tidal range components, but only peaks with periods within the semidiurnal tidal range component are shown (Table 2).

Figure 10 shows the possible relationship between the tide and the 2338 earthquakes events occurred during the reactivation stage or the second stage (P_2) of the post-eruptive phase. Figure 10 A shows the earthquakes that occurred during this seismic reactivation stage. The position of these earthquakes with respect to the tide is reflected in Figure 10 B. Figure 10 C shows the significant periods of swarm P_2 over time. As in Figures 7 C and 9 C, harmonic periods extracted by the spectrum analysis are observed that are as much of the tidal range of the semidiurnal and diurnal tide components. This coincidence of periods with the tide (semidiurnal and diurnal), it is also reflected in Table 2, where swarm P_2 presents significant harmonic peaks with the semidiurnal and diurnal tide range components for M> 0 and M> 1, while for M> 2 only significant harmonic peaks coincide with the semi-diurnal tide range components.

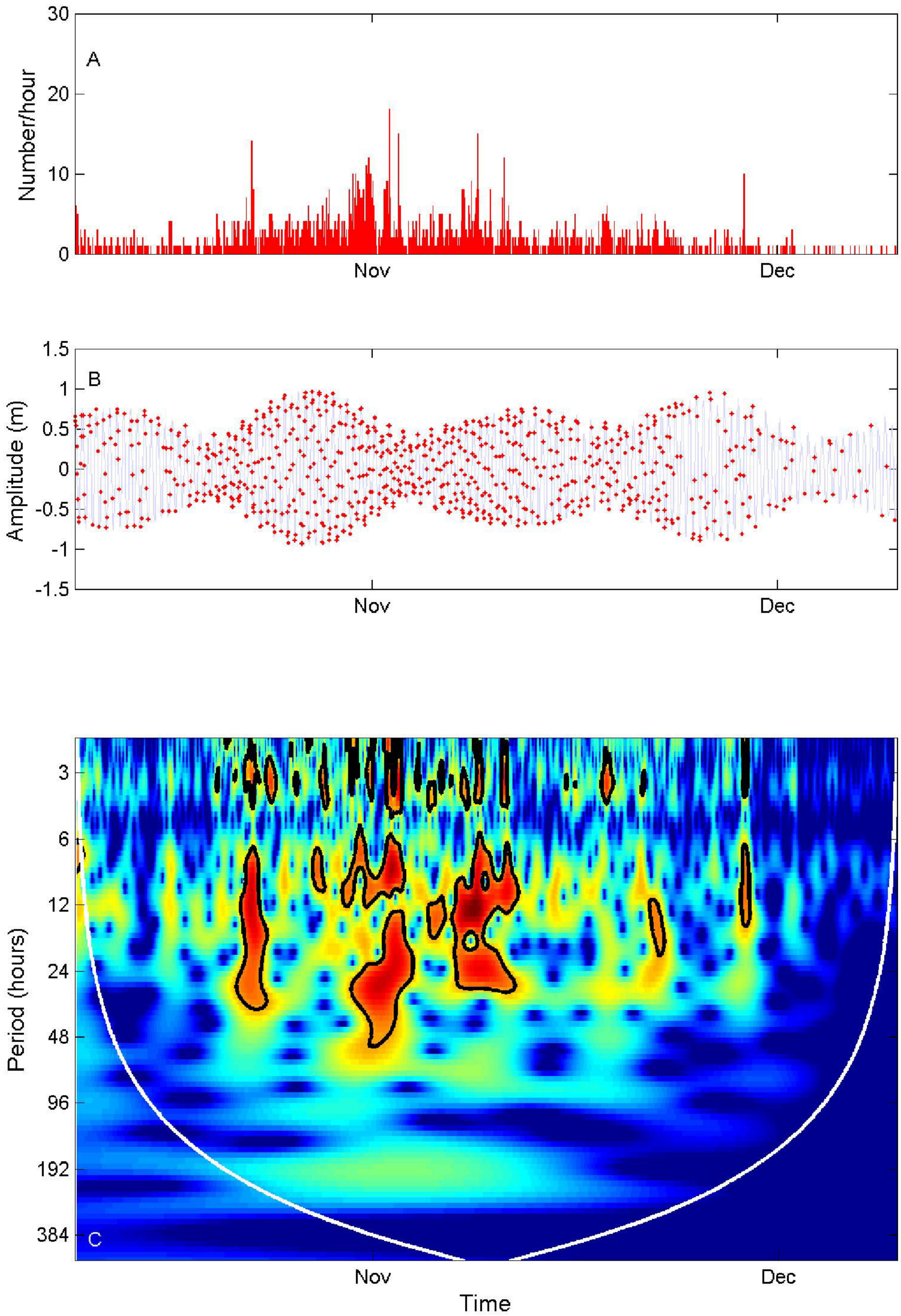

Figure 9: (A) Time series showing the number of seismic events per hours in eruptive stage (swarm Pre_1 from 10/10/2011 to 09/12/2011), (B) distribution of earthquake in the tidal amplitude (m). (C) Result of the application of the wavelet analysis to the filter time series.

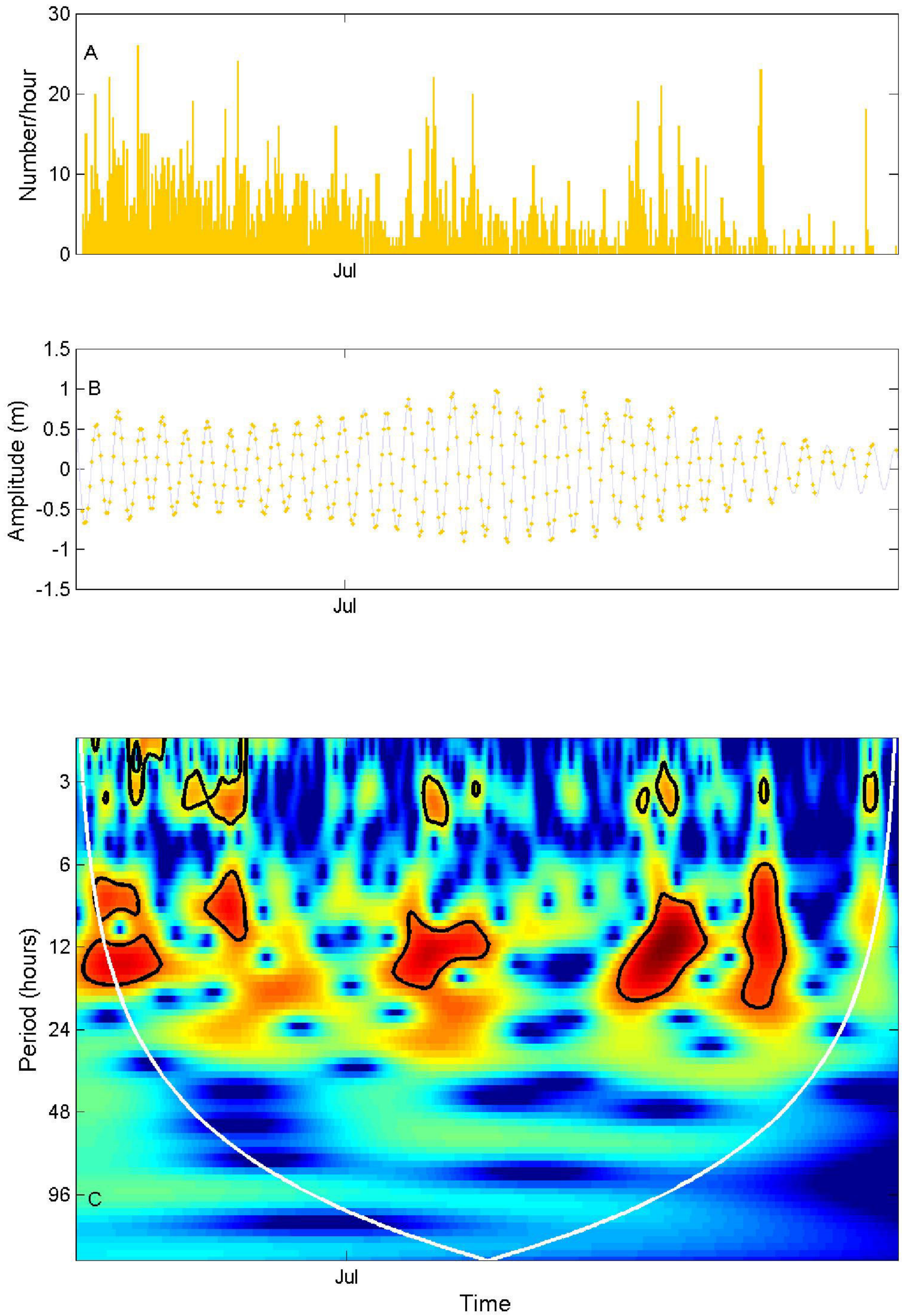

Figure 10: (A) Time series showing the number of seismic events per hours in eruptive stage (reactivation). (B) Distribution of earthquake in the tidal amplitude (m). (C)Result of the application of the wavelet analysis to the filter time series.

6.5. Reconstruction

In order to try to advance in the prediction of the future time series of earthquakes, a reconstruction of the filtered original time series using the significant harmonic period were done for each swarm. The percentage of reconstruction are shown in Table 2.

The reconstruction of the filtered signal was carried out following equation 1, by means of a summation of the harmonic periods with greater significance obtained with the spectral analysis. The reconstruction signals with lower percentage of reconstruction occur during the eruptive stage and the first swarm of the post-eruptive stage. The highest reconstruction percentages were obtained during the pre-eruptive stage (Pre_2), with a 38% of the filtered original signal reconstructed, and during the reactivation stage (P_2) when a 42% of the signal was achieved.

Figure 11 shows the reconstruction of the signal given by the swarm P_2. This signal was reconstructed from the most significant peaks given by the spectral analysis at this swarm. The green line represents the original filtered signal while the red line represents the reconstruction signal with a final reconstructed percentage of 42%

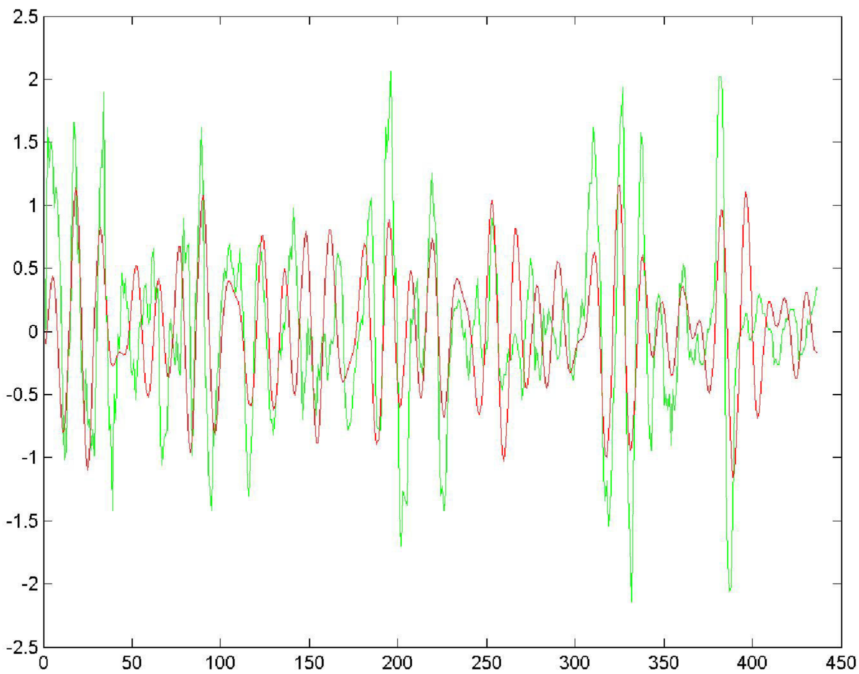

Figure 11: Filter time series of earthquake events for P2 swarm (green line). Reconstruction of the filtered original signal with the significative harmonic period extracted by the spectral analysis shown in Table 2 (red line).

7. Discussion

Although there are many studies on the influence on the tidal on worldwide earthquakes, there are few studies showing this correlation associated with an underwater monogenetic volcano.

Although strong correlation between earthquakes and tides have been confirmed (Mauk & Johnston, 1973; Dzurisin, 1980 and Rydelek, et al., 1988), several authors suggested that earthquakes were produced mainly near the low tide phases (Wilcock, 2001; Tolstoy et al., 2002) when the decrease in confining pressure of part of the weight of the ocean is removed. Nevertheless, our results suggest significant correlations not only for low tide phases but also for high tide phases. The existence of the correlation between earthquakes and the high tide should be due to the increase of the pressure that is generated on the crust.

Tolstoy et al. (2002) and Rydelek et al. (1988) observed correlation between tidal and earthquakes associated to seismic processes as faults, tectonic plates and hot spots. Conversely, tidal influence on earthquakes associated to seismic-volcanic process of monogenetic volcano has never been studied. Our work shows significant correlations for earthquakes with magnitudes $m<3$. This result is similar to that obtained by Rydelek et al. (1988) of the study of the Kilauea volcano (hot spots process) for earthquakes with magnitudes $m<=2$. However, Tolstoy et al. (2002) for the Axial volcano on Juan de Fuca Ridge, and Ide et al. (2016) for Japan, observed also this correlation but only for earthquakes with magnitude $m>6$ and for the great earthquakes in Japan, respectively. Our results are in better agreement with the Kilauea volcano results, may be due that both studies were done over systems that are not related to plates boundaries but to hot-spots.

Rydelek et al. (1988) observed that in the pre-eruptive stage, the reconstruction of the tidal signal is more important than in the eruptive stage. They explain that these results were consequence of the propagation trough of dikes, sills or along conduits in the brittle edifice of Kilauea volcano. So, they proposed that as the pressure builds up in such structures prior to propagation, a near critical stress (tectonic stress) level is reached, above which earthquakes will be generated. In our study the results obtained were similar to those obtained in the Kilauea volcano, because in this work the reconstruction most important were getting in the pre-eruptive stage and in the reactivation stage. That the greatest reconstructions are obtained are these phases is due to the great pressure exerted by the magma on the crust during these stages. In these stages the IGN came to record deformations of over 5 cm.

Rydelek et al. (1988) obtained with the theoretical tide that the semidiurnal tide have more importance than the diurnal tide, but when analyzed this influence or importance of the tide with the real tide, they discovered that the diurnal tide had more importance than the diurnal tide. They explain that the difference found between the analysis with the real and theoretical tide, may be due to the influence of several components as atmospheric pressures, diurnal temperature effects at the surface to extend to depth (Thermoelastic coupling), cultural activity, etc. Our study was only carried out through the theoretical tide, and the results found agree with those found by Rydelek et al. (1988).

8. Conclusion

Earthquakes events were produced constantly in the world, whether produced by process associated with volcanoes or tectonic plates. These types of events are very difficult to predict, for this reason, studies than try to help to predict them are of high relevance. In that way, our study has been carried out related to the recently submarine volcano gave rise in Spain and one of the youngest volcanoes in the world, Tagoro.

Our results highlight, a strong significant correlation (up to 99.99%) between earthquakes events and tide that provides a significant percentage of reconstruction of earthquakes occurrence, getting a reconstruction from 30-42% in several swarms. This correlation has been observed to be more significant during semidiurnal tide events than diurnal tide events. Differences between the correlation obtained over the different stages has also been observed, with maximum correlations during the pre-eruptive and reactivation stages. Moreover, earthquakes events have been observed to be more probable during maximum and minimum peak tides.

9. Future works

The present work studies the correlation in the generation of earthquakes by the tide. For future works will be carried out studies of correlations between earthquakes and other physic parameter as atmospheric pressure, Moon phase, Sun phase, etc., in order to increase the percentage of occurrence of earthquakes and try to optimize as much as possible the possible prediction of this important target.

10. Acknowledgments

This study has been supported by funds from FEDER and the Spanish Ministry of Economy and Competitiveness through the VULCANO-II project (CTM2014-51837-R) lead by the Spanish Institute of Oceanography (IEO). I would like to thank Dra. María

José Blanco from the National Geographic Institute (IGN) that provide the seismic catalog, the IEO to allow me staying during the period of university trainers, to University of Las Palmas de Gran Canaria (ULPGC) that provide the degree and to my two supervisors, Dr. Eugenio Fraile Nuez from IEO and Prof. Dr. Melchor González Dávila from ULPGC for their supports.

11. References

Cooley, J. W., & Tukey, J. W. (1965). An algorithm for the machine calculation of complex Fourier series. *Mathematics of computation*, *19*(90), 297-301.

Curchin, J. M., & Pennington, W. D. (1987). Tidal triggering of intermediate and deep focus earthquakes. *Journal of Geophysical Research: Solid Earth*, *92*(B13), 13957-13967.

Ding, Z. Y., Jia, J. K., & Wang, R. (1983). Seismic triggering effect of tidal stress. *Tectonophysics*, *93*(3-4), 319-335.

Duhamel, P., & Vetterli, M. (1990). Fast Fourier transforms: a tutorial review and a state of the art. *Signal processing*, *19*(4), 259-299.

Dzurisin, D. (1980). Influence of fortnightly earth tides at Kilauea volcano, Hawaii. *Geophysical Research Letters*, *7*(11), 925-928.

Egbert, G. D., Bennett, A. F., & Foreman, M. G. (1994). TOPEX/POSEIDON tides estimated using a global inverse model.

Fraile-Nuez, E., González-Dávila, M., Santana-Casiano, J. M., Arístegui, J., Alonso-González, I. J., Hernández-León, S., Gelado-Caballero, M.D, Eugenio, F.,Marcello, J., de Armas, D., Dominguez-Yanes, J.F, Montero, M.F., Laetsch, D.R., Vélez-Belchí, P., Ramos, A., Ariza, A.V, Comas-Rodríguez, I. &Benítez-Barrios V.M. (2012). The submarine volcano eruption at the island of El Hierro: physical-chemical perturbation and biological response. *Scientific Reports*, *2*, 486.

Frigo, M., & Johnson, S. G. (1998). FFTW: An adaptive software architecture for the FFT. In *Acoustics, Speech and Signal Processing, 1998. Proceedings of the 1998 IEEE International Conference on* (Vol. 3, pp. 1381-1384). IEEE.

Glaser, J. H. (2003). Breathing of the seafloor: Tidal correlations of seismicity at Axial volcano: Comment COMMENT. *Geology*, *31*(1), e3-e3.

Grinsted, A., Moore, J. C., & Jevrejeva, S. (2004). Application of the cross wavelet transform and wavelet coherence to geophysical time series. *Nonlinear processes in geophysics*, *11*(5/6), 561-566.

Hartzell, S., & Heaton, T. (1989). The fortnightly tide and the tidal triggering of earthquakes. *Bulletin of the Seismological Society of America*, *79*(4), 1282-1286.

Hall-Spencer, J. M., Rodolfo-Metalpa, R., Martin, S., Ransome, E., Fine, M., Turner, S. M., Rowley, S.J., Tedesco, D. &Buia, M. C. (2008). Volcanic carbon dioxide vents show ecosystem effects of ocean acidification. *Nature*, *454*(7200), 96-99

Heaton, T. H. (1975). Tidal triggering of earthquakes. *Geophysical Journal International*, *43*(2), 307-326.

Heaton, T. H. (1982). Tidal triggering of earthquakes. *Bulletin of the Seismological Society of America*, *72*(6A), 2181-2200.

Ide, S., Yabe, S., &Tanaka, Y. (2016). Earthquake potential revealed by tidal influence on earthquake size-frequency statistics. *Nature Geoscience*.

Lomb, N. R. (1976). Least-squares frequency analysis of unequally spaced data. *Astrophysics and space science*, *39*(2), 447-462

Mauk, F. J., & Johnston, M. J. S. (1973). On the triggering of volcanic eruptions by Earth tides. *Journal of Geophysical Research*, *78*(17), 3356-3362.

McNutt, S. R., & Beavan, R. J. (1981). Volcanic earthquakes at Pavlof Volcano correlated with the solid earth tide. *Nature*, *294*(5842), 615-618.

Morgan, W. J., Stoner, J. O., & Dicke, R. H. (1961). Periodicity of earthquakes and the invariance of the gravitational constant. *Journal of Geophysical Research*, *66*(11), 3831-3843.

Omori, F. (1908). Notes on the secondary causes of earthquakes. *Bulletin of the Imperial Earthquake Investigation Committee*, *2*(2), 101-135.

Oppenheim, A. V. and Schafer R. W. (1989).Discrete-Time Signal Processing.*Prentice-Hall*, p. 611.

Press W. H, Teukolsky, S.A. Vetterling, W.T. and Flannery, B.P. (2001). Numerical recipes in Fortran 77: the art of scientific computing. *Cambridge University Press, NY, USA*, 2nd ed., *1*.

Rader, C. M. (1968). Discrete Fourier transforms when the number of data samples is prime. *Proceedings of the IEEE*, *56*(6), 1107-1108.

Resing, J. A., Baker, E. T., Lupton, J. E., Walker, S. L., Butterfield, D. A., Massoth, G. J., & Nakamura, K. I. (2009). Chemistry of hydrothermal plumes above submarine volcanoes of the Mariana Arc. *Geochemistry, Geophysics, Geosystems*, *10*(2).

Rydelek, P. A., Davis, P. M., & Koyanagi, R. Y. (1988). Tidal triggering of earthquake swarms at Kilauea volcano, Hawaii. *Journal of Geophysical Research: Solid Earth*, *93*(B5), 4401-4411.

Santana-Casiano, J. M., González-Dávila, M., Fraile-Nuez, E., De Armas, D., González, A. G., Domínguez-Yanes, J. F., & Escánez, J. (2013). The natural ocean acidification and fertilization event caused by the submarine eruption of El Hierro. *Scientific reports*, *3*, 1140.

Santana-Casiano, J. M., Fraile-Nuez, E., González-Dávila, M., Baker, E. T., Resing, J. A., & Walker, S. L. (2016). Significant discharge of CO2 from hydrothermalism associated with the submarine volcano of El Hierro Island. *Scientific reports*, *6*, 25686.

Schuster, A. (1897). On lunar and solar periodicities of earthquakes. *Proceedings of the Royal Society of London*, *61*(369-377), 455-465.

Simpson, J. F. (1967). Earth tides as a triggering mechanism for earthquakes. *Earth and Planetary Science Letters*, *2*(5), 473-478.

Tsuruoka, H., Ohtake, M., & Sato, H. (1995). Statistical test of the tidal triggering of earthquakes: contribution of the ocean tide loading effect. *Geophysical Journal International*, *122*(1), 183-194.

Torrence, C., & Compo, G. P. (1998). A practical guide to wavelet analysis. *Bulletin of the American Meteorological society*, *79*(1), 61-78.

Tolstoy, M., Vernon, F. L., Orcutt, J. A., & Wyatt, F. K. (2002). Breathing of the seafloor: Tidal correlations of seismicity at Axial volcano. *Geology*, *30*(6), 503-506.

Wilcock, W. S. (2001). Tidal triggering of microearthquakes on the Juan de Fuca Ridge. *Geophysical Research Letters*, *28*(20), 3999-4002.

MEMORIA FINAL DEL TRABAJO DE FIN DE GRADO (TFG)

GRADO EN CIENCIAS DEL MAR. ASIGNATURA:40630-Trabajo de Fin de Título

Año académico: 2016-2017 Alumno: Atenary Pimentel González

1. Descripción detallada de las actividades desarrolladas durante el TFG

Para la realización del TFG, el investigador responsable marco una serie de actividades a seguir, las cuales fueron revisadas por el tutor académico. Estas actividades fueron las siguientes:

1.1 Reunión inicial. Planificación y temporalización

Durante la primera semana se llevó a cabo una serie de reuniones en las cuales se acordó que el TFG se realizaría en conjunto con las prácticas de empresa en un periodo de 5 meses (Enero a Mayo), el cual fue ampliado posteriormente hasta el mes de Junio. En estas reuniones también se realizó una planificación y temporalización de cada una de las actividades que se iba a realizar para el desarrollo del TFG, y también se nos informó de las herramientas que se iban a utilizar.

1.2 Lectura de bibliografía específica

Durante dos semanas se llevó a cabo una lectura cuidadosa de los artículos previamente seleccionados. Tras realizar una primera lectura de cada uno de los artículos científicos los debatía con mi tutor para así solucionar todas las dudas que me iban surgiendo a medida que realizaba la lectura de los artículos.

1.3 Obtención, procesado y graficado de los datos

Para este TFG se utilizaron datos de terremotos y de marea que tuvieron lugar durante el periodo sismo eruptivo de la isla de Hierro durante el 01-01-2011 hasta 31-07-2012.

El catálogo de terremotos fue proporcionado por el Instituto Geográfico Español (IGN), mientras que los datos de marea fueron obtenidos mediante un modelo matemático denominado marea TPXO7.2ATLAS (Egbert, Bennett, & Foreman, (1994). TOPEX / POSEIDON).

El procesado y el graficado de los datos se realizó bajo entorno Matlab. Para llevar a cabo estas tareas se usaron modelos matemáticos específicos como la FFT (Cooley and Tukey, 1965; Rader, 1968; Oppenheim & Schafer, 1989; Duhamel & Vetterli, 1990; Frigo & Johnson, 1998), la Fastlomb, (Lomb (1976); Press et al, 2001y la CWT, Continuous Wavelet Transform (Torrence & Compo, 1998; Grinsted et al., 2004).

1.4 Redacción del TFG

El TFG se realizó con formato de artículo científico, en el cual se desarrollaron los siguientes apartados:

-Motivación
-Backgraund
-Introducción
-Material y métodos
-Resultados
-Discusión y
- Conclusión

2. Formación recibida (Cursos, programas informáticos, etc)

Formación recibida: Curso certificado en programación de lenguaje en matlab en el ámbito de la oceanografía. Además adquirí nuevos conocimientos en oceanografía que no se dieron durante la carrera, como técnicas específicas para obtener resultados de una base de datos reales. Algunas de estas técnicas específicas fueron aplicar diferentes métodos como la Wavelet, la Transformada de Fourier, aplicar filtros a una serie temporal de datos, etc.

Programas: Durante las prácticas utilicé programas como el Word, Powerpoint, Excel y Matlab.

3. Nivel de integración e implicación dentro del departamento y relaciones con el personal

El nivel de integración dentro de la empresa fue grato, ya que mantenía una relación cordial con todos los miembros del departamento. Además, tenía toda la libertad para usar las instalaciones presentes en el IEO como el parking cafetería, etc.

4. Aspectos positivos y negativos más significativos relacionados con el desarrollo del TFG

Aspectos positivos:

- Trabajar con datos reales sin publicar relacionados con uno de los proyectos más novedosos y llamativos del centro oceanográfico canario.
- Perfeccionar la técnica de redactar un artículo científico.
- Aprender y perfeccionar el manejo en un lenguaje matricial científico muy importante en la oceanografía como es el Matlab.
- Trabajar en una de las principales instituciones dedicada a la oceanografía en el territorio español.
- Posibilidad de asistir a conferencias de comités científicos que se realizan en el centro oceanográfico de canarias.

5. Valoración personal del aprendizaje conseguido a lo largo del TFG

El aprendizaje conseguido durante el desarrollo del TFG fue positivo, ya que aplique cierto de los conocimientos obtenidos durante la carrera durante la realización del TFG. Además de perfeccionar las diferentes técnicas de escrituro que se aplican al redactar un artículo científico.